

Delineating weak zones in limestone based on borehole drilling and electrical resistivity tomography

Muhammad Jahangir Khan¹, Siddique Akhtar Ehsan^{2,*}, Umair Bin Nisar³,
Syed Shahrukh Ali¹, Mubarak Ali¹, Hummad Habib Qazi⁴, Saif-ur-Rehman⁵, Sarfraz Khan⁶

¹*Dept. of Earth & Environmental Sciences, Bahria University,
Karachi Campus, Pakistan*

²*Dept. of Physics, COMSATS University Islamabad, Lahore Campus, Pakistan*

³*Centre for Climate Research and Development, COMSATS University Islamabad, Pakistan*

⁴*Innovative Eng. Research Alliance, University Teknologi Malaya, Johar, Malaysia*

⁵*Key laboratory of Continental Collision and Plateau Uplift,*

Institute of Tibetan Plateau Research, Chinese Academy of Sciences, Beijing, China

⁶*National Center for Excellence in Geology, University of Peshawar, KPK, Pakistan*

** Corresponding author: siddiquemir1@gmail.com*

Abstract

This study is focused on imaging weak zones in the subsurface using borehole and geophysical datasets. These weak zones are present within the Jhill limestone of the Miocene age across northern Karachi. A total of forty-nine core samples were collected from eleven boreholes about 30 m deep within the study area. The core analysis reveals the presence of cavities in fractured limestone at shallow and deep levels. The lateral extension and thickness of these weak zones are well imaged by the electrical resistivity tomography (ERT) dataset. The 2D tomographs of the six profiles show variability in the ground resistivity response. The ERT profiles are interpreted using on-hand samples collected from boreholes. These tomographs reveal relatively high resistivity values interpreted as intercalation of dry clay and marl beds within the limestone. The medium resistivity values suggest the presence of clay and sand in highly fractured limestone or surficial dry features. The low resistivity values are interpreted to be originated from the weak zones filled with lithologies having high moisture content within the limestone. The collected core samples were analysed for geotechnical parameters. The integration of borehole and ERT datasets delineated weak zones in the northern and central regions, which should be well-cemented to avoid any geohazard.

Keywords: Borehole data; electrical resistivity tomography; limestone; resistivity; weak zones.

1. Introduction

Under the influence of rapid urban developments of towns and cities, it is pertinent to locate safe ground for construction to avoid any potential geohazard. The potential geohazards for civil structures may include earthquakes, volcanic activity, tsunamis, landslides, floods, and the presence of weak zones in the subsurface. Although the massive beds of limestone are recognized

as a stable platform, however dissolution character of the carbonate rocks in the presence of the acidic groundwater may cause voids, cavities/weak zones, sinkholes, and caverns which are considered sensitive zone for mega-construction projects (Zhu *et al.*, 2011; Cueto *et al.*, 2018; Butchibabu *et al.*, 2019).

The most common procedures for assessing ground stability conditions include drilling boreholes, geophysical measurements, and geotechnical studies (Khan & Ali, 2020). Besides the wide spectrum of geophysical studies, the electrical resistivity tomography (ERT) helps investigate such anomalies in the subsurface (Hussian *et al.*, 2017; André *et al.*, 2016; Li *et al.*, 2020). The ERT method reveals horizontal and vertical discontinuities in terms of the electrical properties of the shallow subsurface (Alle *et al.*, 2018; Ewusi *et al.*, 2009). Although the identification of the dissolution features in the subsurface is a real challenge, ERT delineations produce better results to address the influence of anisotropic medium, heterogeneity in physical properties, and derivatives of dimensions in shallow subsurface ((Zhu *et al.*, 2011; Redhaounia *et al.*, 2016; Kearey *et al.*, 2002). The main advantage of the ERT and drilling data combination is the calibration of the electrical resistivity measurements in shallow environments.

The geotechnical estimation of core samples provides local ground stability conditions at a centimeter scale (Tao *et al.*, 2018b; Khalil & Hanafay, 2016). The geotechnical parameters that include natural moisture content, dry density, bulk density, and specific gravity are usually considered to determine subsurface rock conditions which contribute to the safe foundation design of buildings, bridges, and mega infrastructures (Régnier *et al.*, 2016). The geotechnical analysis of core samples may be coupled with the ERT results to reveal anomalous zones and substrate conditions at high resolution (Khalil & Hanafay, 2016; Rasul *et al.*, 2018). In this study, we have focused on the identification of voids/weak zones in the shallow subsurface across the Jhill limestone.

2. Study area

Karachi city is expanding in its outskirts. There are aforementioned concerns of the surveyors and town developers regarding safe constructions and the identification of anomalous pockets in the subsurface. The current study is carried out across Jhill limestone outcrops located about 55 km northeast of Karachi (Figure 1a). The study area spreads over 34706 m² (8.58 Acres), and it is covered by moderate hilly sedimentary rocks about 600 m above the mean sea level (Figure 1b). Thereby sedimentary outcrops mainly consist of limestone interbedded with shale, siltstone, and sandstone of the Gaj Formation of the Miocene age in the Karachi region (Shah, 2009). The Jhill limestone is a thick carbonate deposit of the Gaj Formation, which was deposited in the shallow marine environment and is partly recrystallized (Figure 2).

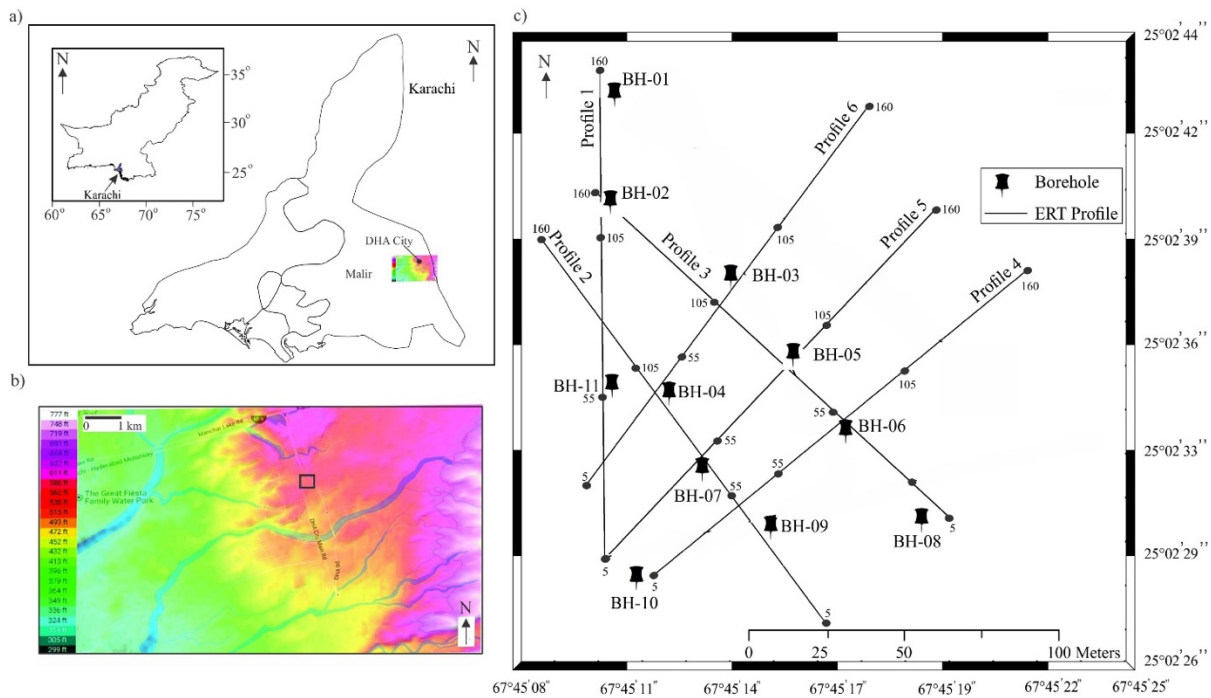


Fig. 1. a) Geographical map of Pakistan. Karachi is highlighted on the onset of the map, b) the Topographic map of the study area and its surroundings, and c) Basemap of electrical resistivity profiles and boreholes in the study area.

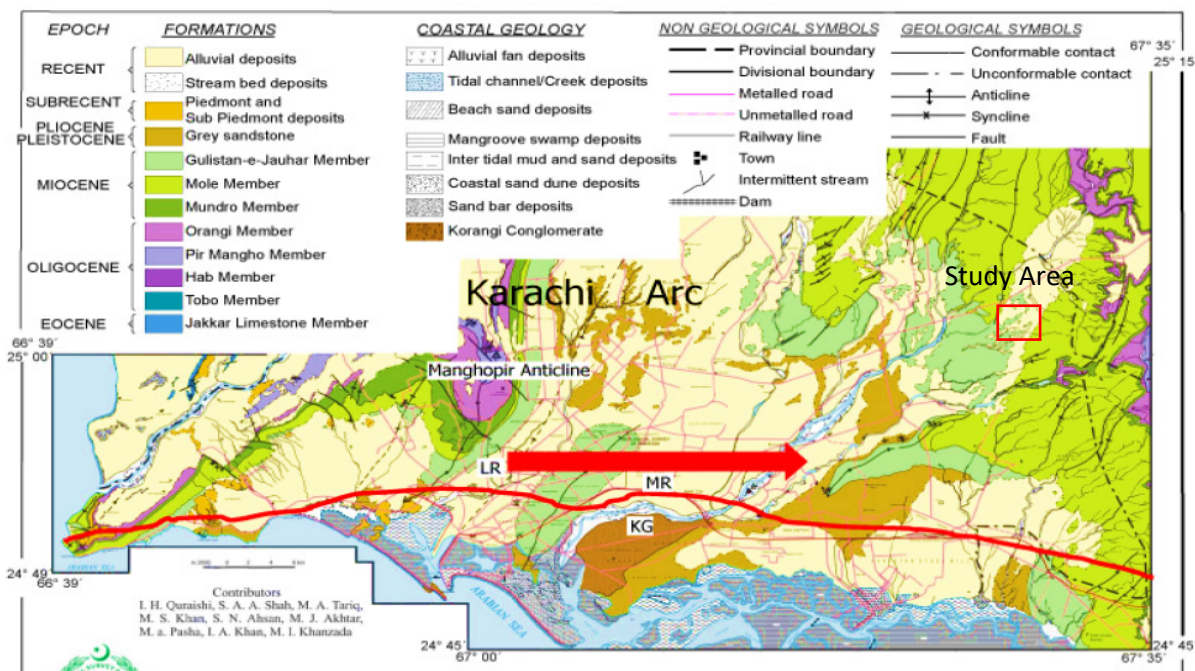


Fig. 2. Geological map of Karachi City and its surroundings. The red rectangle shows the location of the study area (Modified after Quraishi *et al.*, 2001).

3. Data acquisition and processing

3.1 Borehole data

A total of eleven boreholes of about 10 cm diameter were drilled, ranging in depth from 25 m to 45 m (Figure 1c). The boreholes were drilled with a straight rotary rig having an HQ double tube core barrel. This technique produced continuous soil and rock cores samples. About forty-nine core samples were preserved in the core boxes for laboratory examination of the natural moisture content, dry density, bulk density, and specific gravity. The presence of cavities was evident during the drilling operation.

3.2. Geophysical data

The ERT survey was carried out using a composite Wenner-Schlumberger configuration across the study area (Figures 3a and 3b). The six ERT profiles (Profile-1 to Profile-6) run in a grid manner across a reworked flat soil cover in the vicinity of undulating limestone beds (Figure 1c). 2D ERT data acquisition was conducted using POLARES 2.0, in which thirty-two electrodes were connected at 5 m intervals to a profile of cover 160 m. The electrodes inserted in the ground are connected through a wire to the link boxes and the recording system. The link boxes were connected to the main instrument through box to box cables. After completing the first test, the next profile was acquired utilizing the same acquisition parameters. The acquired 2D ERT data were pre-processed with the help of POLARES utility software. The noises were removed from the raw ERT data. The ERT data were imported to inversion software “RES2DINV” for further iterative processing. The ERT profiles show subsurface resistivity contrast, which helps analyze the heterogeneities.

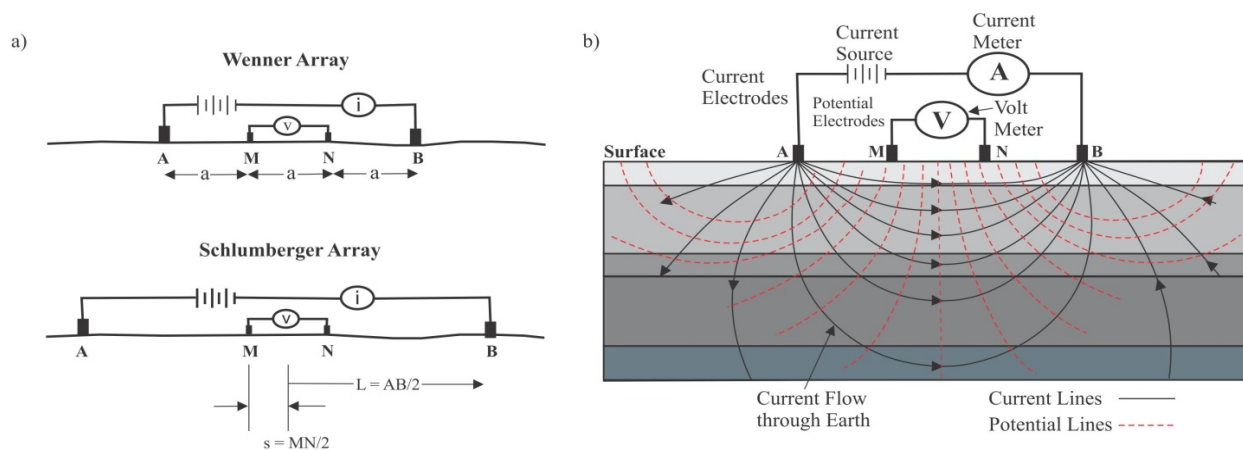


Fig. 3. a) Schematic illustration of the electrode configurations Wenner (Top) and Schlumberger (Bottom). AB represents the spacing between current electrodes, and MN represents the spacing between potential electrodes. b) Schematic illustration of the basic measurements using the electrical resistivity method. Solid black lines represent current flow through the layered subsurface structure and dashed red lines contour electrical potential.

(Modified after Robinson & Coruh, 1988).



Fig. 4. a) Preserved core samples of drilled boreholes in the study area.
b) a single core sample.

4. Results and discussion

4.1 Geological analysis

This borehole data is utilized to constrain the subsurface lithologies, presence of voids, and tying with ERT profiles interpretation across the study area. Based on eleven boreholes (BH-01 to BH-11), three cross-sections (A-A', B-B,' C-C') are prepared (Figures 5a, 5b, and 5c). The cross-section A-A' was generated from boreholes BH-08, 06, 05, and 03 to reveal the extent of limestone and minor lithologies. The cross-section A-A' reveals that the top layer consists of yellowish-brown fine to coarse grain sand with gravel. This layer varies in thickness from about 2.5 m in the northwest to 1 m in the southeast. These are the recent depositions associated with the stream fluctuations. The prominent layer encountered during drilling is fractured limestone, about 27 m thick (Figure 5a). The presence of thick limestone is evident across the A-A'; however, intercalation of thin claystone layer is encountered at about 17 m depth and 28 m in BH-06 and 08, respectively. The boreholes (BH-03 and 05) drilled in the central part of the study area which shows the presence of cavities at about 12 m depth. The boreholes (BH-06 and 08) drilled in the south show no sign of voids/weak zones in the limestone. The ERT Profiles-6, 5, and 4 run cross-sections A-A' from north to south (Figure 5a).

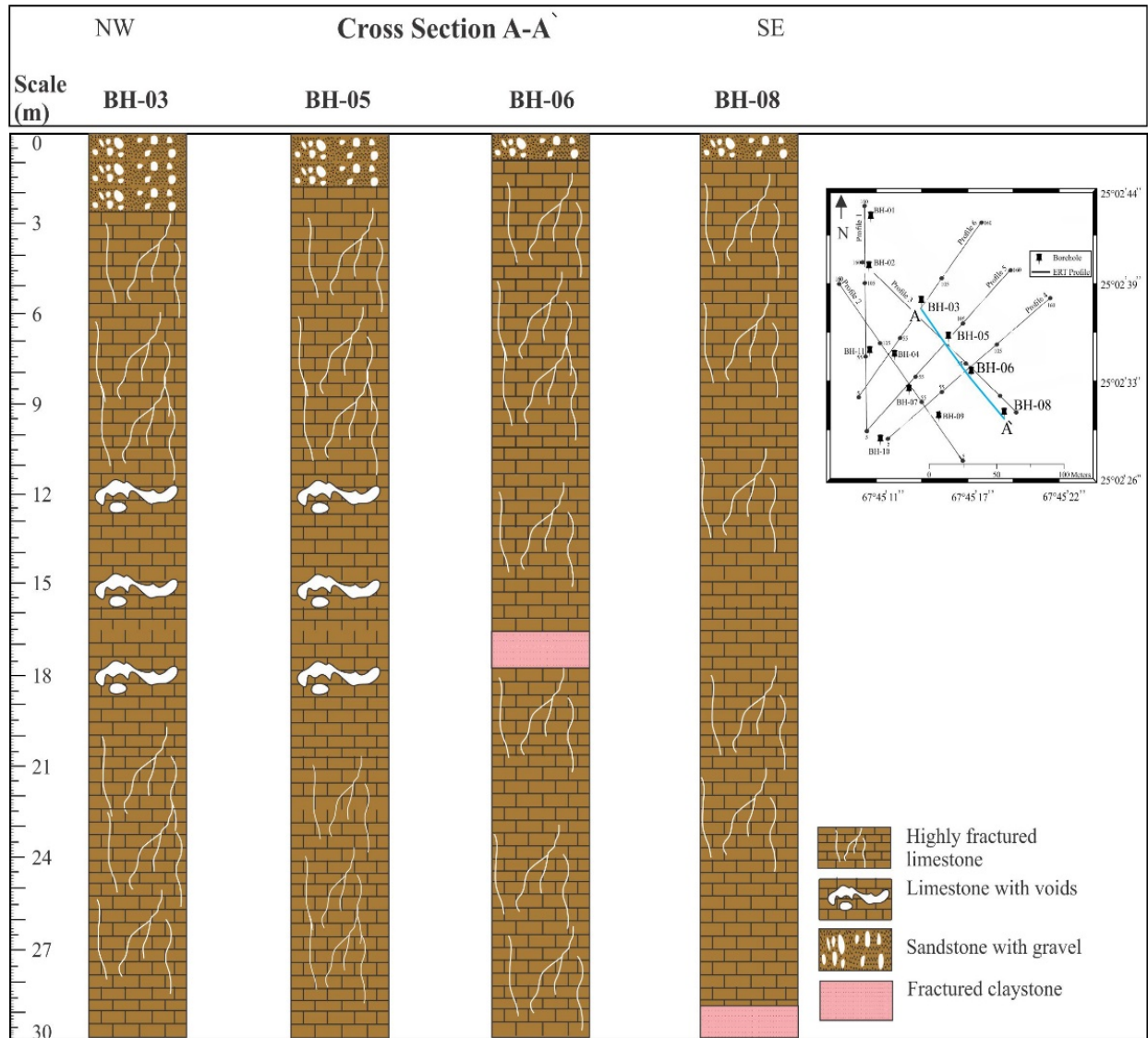


Fig. 5. a) Cross Section A-A' shows a correlation between four boreholes.

The location of the Cross Section A-A' is highlighted in the onset of the map with a blue line.

The cross-section B-B' consists of three boreholes (BH-04, 07, and 09) and reveals a fractured and weathered massive limestone layer having a total thickness of 29 m. The presence of voids in limestone is only evident in BH-04 from a depth ranging from 10 m to 14.5 m in the northwest. The intercalation of the thin claystone layer in fractured limestone is evident in the southeast at about 2 m and 17 m depths. These lithological variations correspond to stream fluctuation due to subaerial exposure of deposited limestone. The boreholes (BH-07 and 09) drilled in the southwest shows no sign of voids/weak zones in the limestone. The ERT Profiles-2, 5, and 4 runs across cross-sections B-B' (Figure 5b).

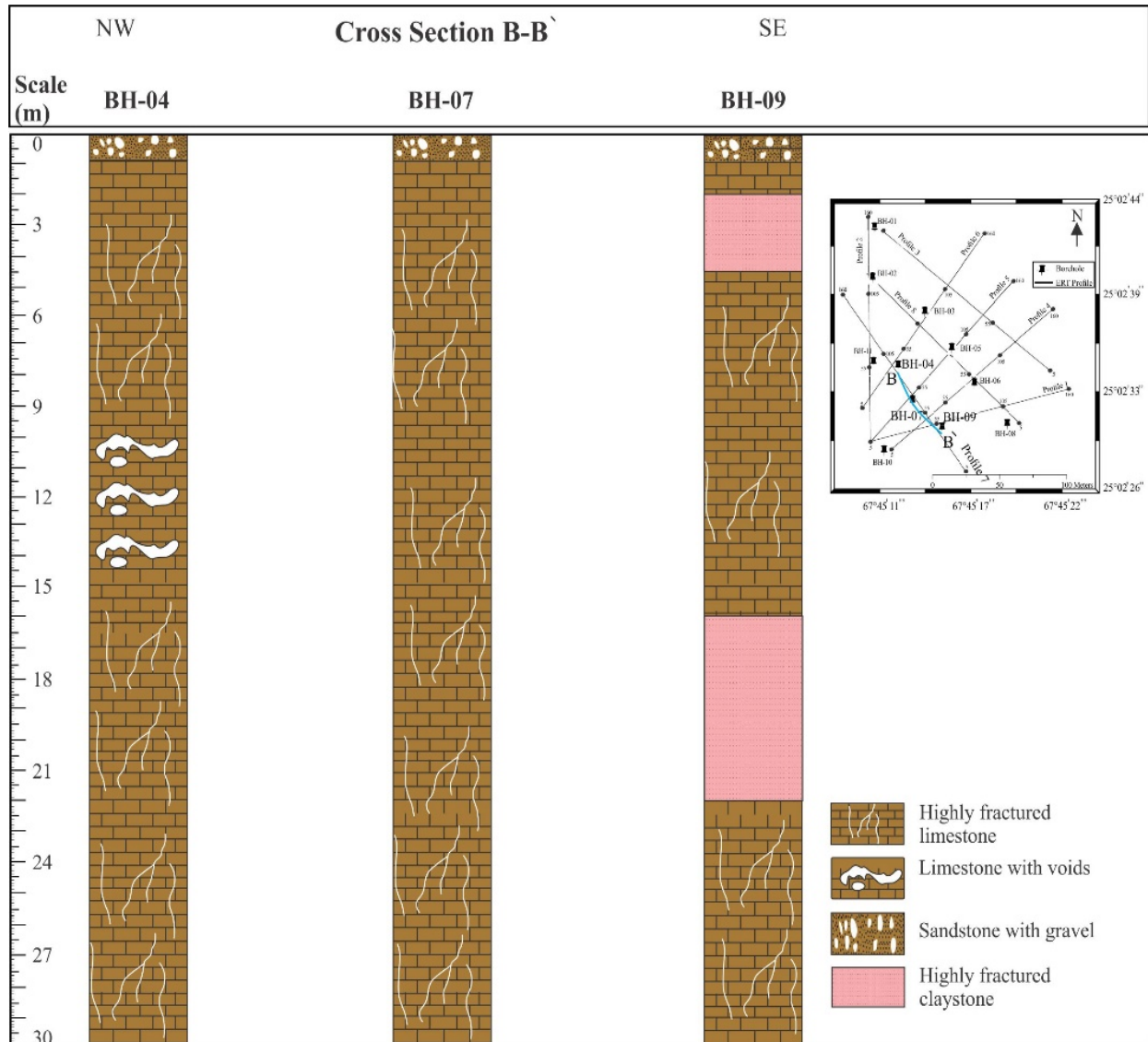


Fig. 5. b) Cross Section B-B' shows a correlation between three boreholes. Location of the Cross Section B-B' is highlighted in the onset of the map with a blue line.

The cross-section C-C' was generated from boreholes (BH-01, 02, 11, and 10) and reveals the presence of variable lithologies (Figure 5c). A remarkable limestone layer about 20 m thick and highly fractured in the south is evident across C-C'. The presence of filled voids, depths ranging from 3 m down to 16 m, is evident from BH-01 in the north. The BH-02 shows the presence of unfilled voids at a similar depth; however, intercalation of thin clays and marls is also evident. The BH-11 and 10 reveal no sign of voids to the south. Two alternative layers of claystone interbedded with sand and sandstone interbedded with clay about 5 m in thick are presence with limestone layers. The ERT Profile-1, 6, and 5 runs across the cross-section C-C' from north to south (Figure 5c).

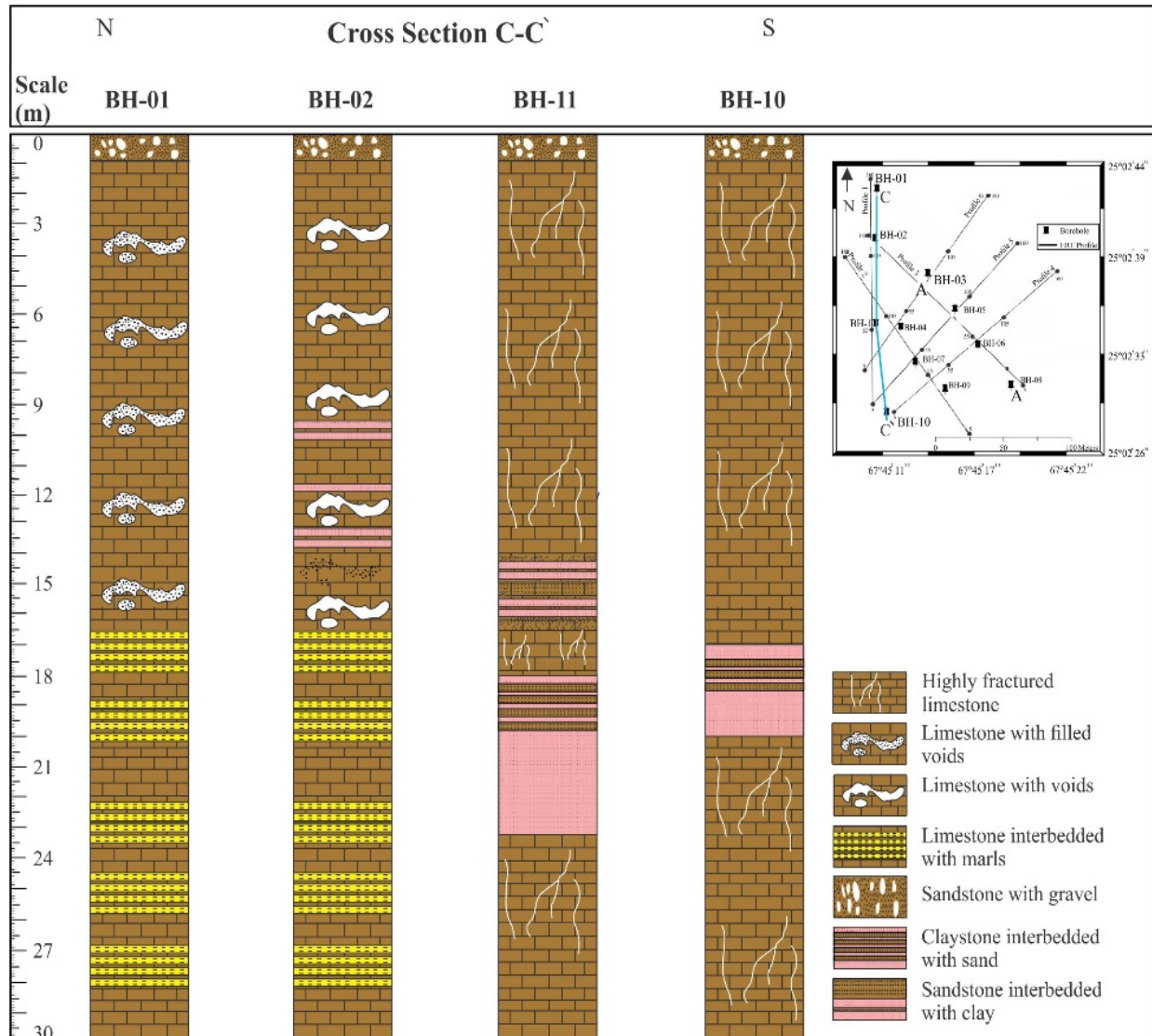


Fig. 5. c) Cross Section C-C' shows correlation between four boreholes (BH-01, BH-02, BH-11, and BH-10). Location of the Cross Section C-C' is highlighted in the onset map.

4.2. Electrical Resistivity Tomographs

The ERT results were interpreted by considering the lithological information obtained from the borehole data. For instance, if a direct measurement of lithology from drilling indicates the presence of a lithology with certain properties from the surface up to 10 m in-depth and in the same depth range, the ERT is showing a resistive body; therefore, it is logical to make the association of lithology and resistivity. This association is applied to different lithologies encountered across all the boreholes. However, the lithologies may vary due to subsurface weathering intensity; as it increases, the resistivity values decrease.

The ERT Profiles-1 to 6 show a range of resistivity values which are subdivided into three sections attributing to variations in lithologies (Table 1). In particular, the ERT profiles are interpreted through analysis of lithologies encountered in the boreholes and resistivity classification of respective lithology.

Table 1. Resistivity values assigned to sedimentary packages based on the VES results.

Lithology	Resistivity (Ωm)
Filled voids in limestone with moisture content	250-1000
Fractured limestone	1000-3000
Dry limestone	3000

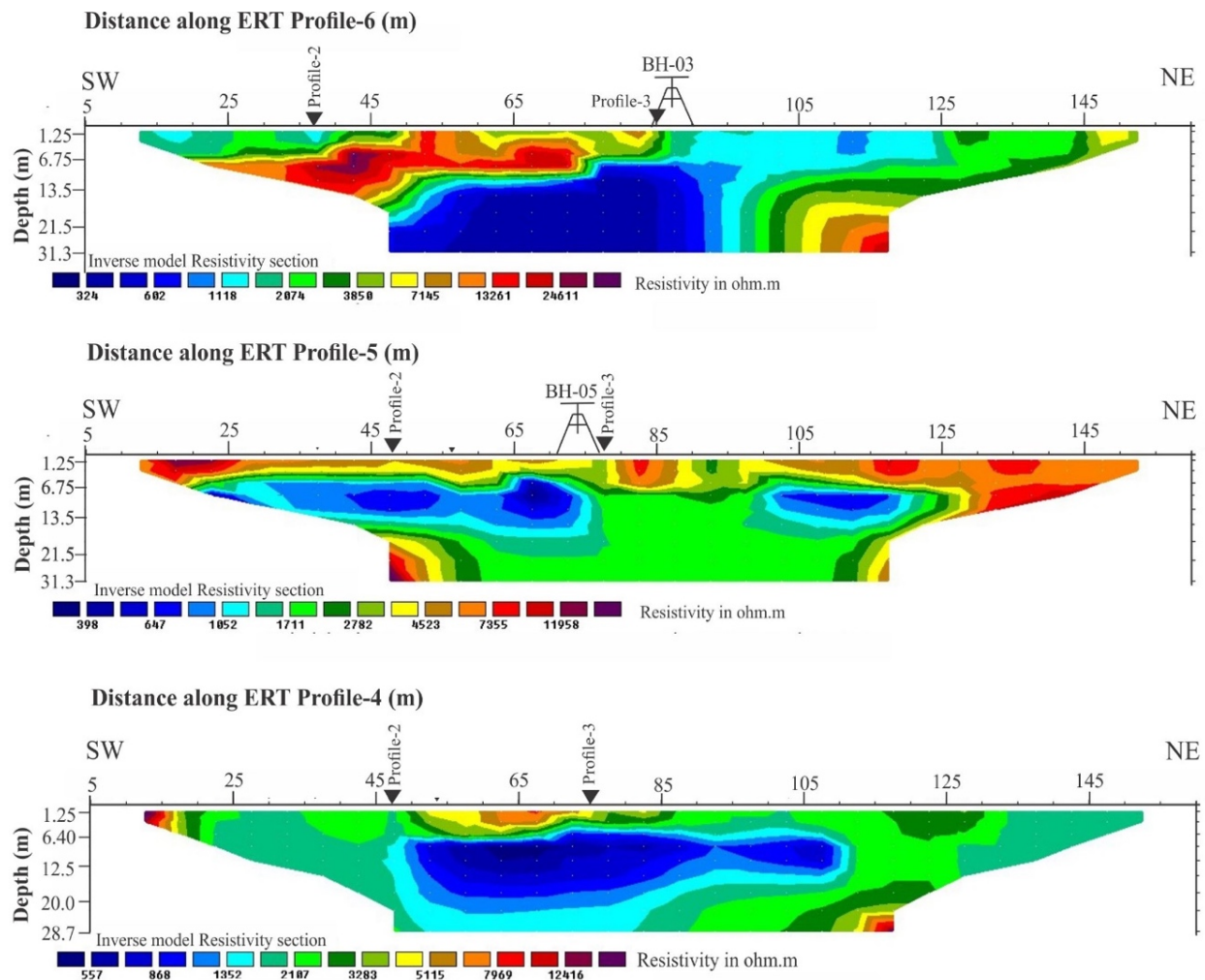


Fig. 6. a) The Electrical Resistivity Tomographs (ERT) were acquired across the study area. The locations of the drilled boreholes are also highlighted on the profiles.

The ERT Profiles-4, 5, and 6 run northeast to southwest (Figures 1c, and 7a). The ERT Profile-6 reveals resistivity values ranging from 300 Ωm to 25000 Ωm . A high resistive zone, values ranging from 7000 Ωm to 25000 Ωm , between distances 20 m to 70 m at about 8 m depth. This zone is interpreted as the intercalation of marl in the fractured limestone. A medium resistivity zone (1600 Ωm to 4000 Ωm) between distances 95 m to 145 m is attributed to dry clay-filled into the fractured limestone down to 32 m depth. The borehole (BH-03) drilled across Profile-6 reveals the presence of voids at about 10 m depth. A loss of about 100-liter drilling fluid was observed while the drilling operation of the BH-03, which may also be due to fractured limestone. A low resistive zone (250 Ωm to 1000 Ωm) between distances 45 m to 90 m and at about 10 m depth is present at the location of voids encountered in the BH-03. However, the water loss during drilling of BH-03 along this void was not observed below 18 m depth. This may suggest filling of this particular voids at a depth greater than 18 m. This low resistive zone present in the Profile-6 and two other parallel profiles (Profile-5 and Profile-4) may represent its extension as a major void in the subsurface.

The ERT Profile-5 shows resistivity values ranging from 350 Ωm to 12000 Ωm , subdivided into three distinct zones (Figure 6a). The borehole (BH-05) drilled in the center of the Profile-5 indicates the presence of dry sand and gravel deposits. A shallow high resistive zone (4000 Ωm to 12000 Ωm) spreads throughout the profile, constrain the presence of surficial dry sand and gravel deposits also indicated by the lithologies in BH-05. An intermediate resistivity zone, between distances of 45 m to 125 m at about 7 m depth, is characterized as fractured limestone interbedded with silt and clay. The image reveals the presence of two low resistive zones, values ranging between 300 to 1050 Ωm , between distances 30 m to 75 m and 100 m to 120 m at about 10 m depth. These low resistive zones can be classified as voids within limestone filled with saturated clay, which are ascertained with BH-05. This may also indicate extension and bifurcation of major voids encountered in Profile-6 from northwest to southeast. The ERT Profile-4 reveals two remarkable resistivity zones, such as between distances 25 m to 130 m at shallow and deeper levels are identified as fractured limestone and between distances 50 m to 110 m at about 7 m depth. This zone represents the subsurface voids within limestone filled with saturated clay.

The ERT Profile-1 runs north-south, and it is located on the western side of the study area (Figure 1c). Three boreholes (BH-01, 02, 11) were drilled across Profile-1. The tomograph of the Profile-1 shows resistivity values ranging from 500 Ωm to 8000 Ωm (Figure 6b). The high resistive zones are interpreted between 100 m to 115 m and 125 m to 140 m at shallow depths, which may be attributed to fractured limestone filled with sand and dry clayey silt in the fractures. The medium resistive zones between distances 30 m to 50 m, 65 to 90 m, and 115 m to 125 m are interpreted to be limestone with high fractured density interbedded with claystone. The BH-01 and 02 identified voids at about 3 m depths (Figure 6c). A low resistive zone between distances of 90 m and 125 m at about 3 m depth constrains the presence of a major voids of about 17 m as identified in BH-01 and 02 (Figure 6b).

The ERT Profiles-2 and 3 run northwest to southeast and parallel to each other (Figure 1c). The tomograph of the ERT Profile-2 image is about 29 m deep and reveals four main features

based on the resistivity values (Figure 6a). A high resistive zone is imaged between distances of 40 m and 75 m, starting at shallow depth and extending down to 16 m depth is interpreted to be intercalations of clay and marl with fractured limestone. Similar, high resistivity values are also observed between distances of 78 m to 128 m at shallow levels, which is interpreted as surficial dry clay. A medium resistive zone is present between distances 70 m to 115 m at about 18 m depth which is attributed as fractured limestone. The BH-04 identified the presence of voids at about 9 m deep. Two low resistive zones are present between 75 m and 90 m and 104 m to 124 m at about 9 m depth. These zones are interpreted as voids in the subsurface.

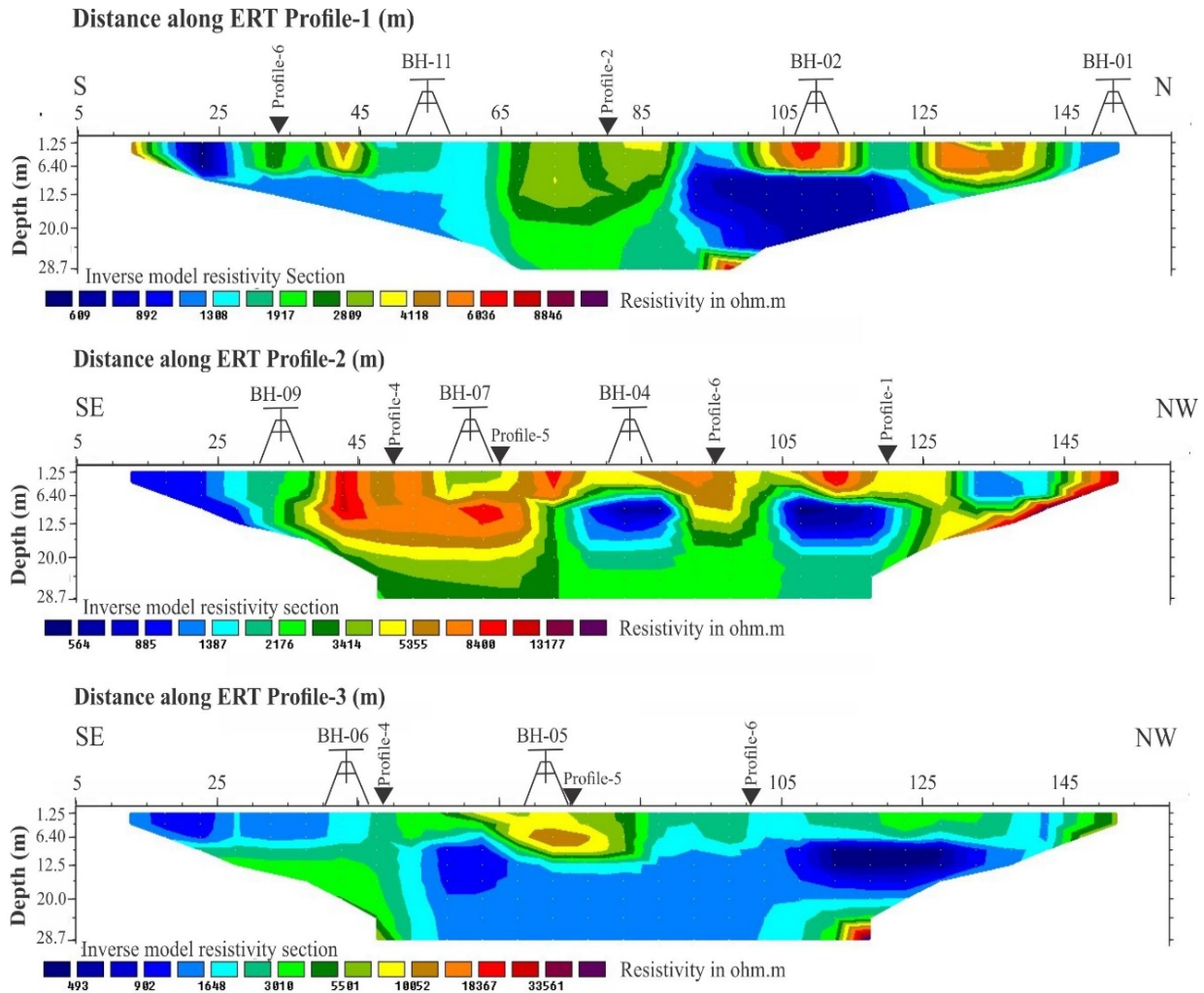


Fig. 6. b) The Electrical Resistivity Tomographs (ERT) were acquired across the study area. The color variations show the resistivity contrast of the subsurface across the profiles. The locations of the drilled boreholes are also highlighted on the profiles.

The ERT Profile-3 (Figure 6b) shows a high resistive zone between distances of 60 m to 75 m at shallow levels. This high resistive zone is located at BH-05 and is attributed to be surficial dry clay. Profile-8 reveals at least three medium resistive zones, values ranging from 2000 to 5500, between distances 45 m to 60 m, 75 m to 100 m, and 108 m to 137 m at shallow levels. These medium resistive zones are interpreted as fracture limestone. The BH-05 encountered voids at about 12 m depth. A low zone resistive zone between distances 55 m to 130 m at about 12 m depth is interpreted as a weak zone in limestone. This is a major zone imaged across the Profile-3. This zone has a lateral extension of about 70 m and goes down to 29 m depth. The Profile-8 also shows two relatively low resistive zones located between distances of 10 m to 45 m at a shallow level. The BH-06 is located between distances of 40 m to 45 m (Figure 6b) and encountered a thickly bedded limestone with intercalation of saturated marls. These low resistive zones constrain the presence of limestone with intercalation of marl from surface to 20 m depth.

4.3. Integration between ERT delineations and geotechnical parameters

The lithology encountered in the eleven boreholes, BH-01 to BH-11, is dominantly limestone with intercalations of marls, clay, silt, sand, and gravel. A reasonable correlation is carried out between the ERT dataset and geotechnical parameters, including moisture content, dry density, bulk density, and specific gravity estimated from the core samples at variable depths (Table 2). The geotechnical parameters are correlated with resistivity values to provide a better understanding of the behavior of different parameters with depth (Table 2). The bulk density shows higher values, 2.15 g/cm³ to 2.13 g/cm³, at a shallow level and low values, 2.1 g/cm³, within the voids zone. The specific gravity shows comparatively higher values for shallow levels, 2.682 to 2.684, and low values, 2.671, for the voids zone. Below the voids, zone-specific gravity reveals the highest value of 2.697 (Table 2). These values suggest a close relationship between geotechnical parameters and electrical resistivity. An inverse relationship between the moisture content and electrical resistivity is observed. At a shallow level, high electrical resistivity and comparatively high values of geotechnical parameters are present. This may indicate the presence of surficial dry clay within fractured limestone at shallow levels. The decrease of resistivity values and geotechnical parameters for depths greater than 7 m suggest filling identified voids with saturated clay or sand. The increase in resistivity and geotechnical parameters for depths greater than 18 m may indicate compaction of the fractured limestone. A similar relationship between geotechnical parameters and electrical resistivity values is present for the remaining four boreholes (BH-02 to BH-05), in which voids have been identified (Table 2).

Table 2. Geotechnical parameters estimated from core samples taken from boreholes

Borehole No.	Sample Depth (m)	Moisture Content (%)	Dry Density (gr/cm ³)	Bulk Density (gr/cm ³)	Specific Gravity
BH-01	3.31	4.07	2.07	2.15	2.682
	6.9	3.74	2.05	2.13	2.684
	12.73	3.73	2.03	2.1	2.671
	24.84	5.6	2.13	2.25	2.697
BH-02	1.6	0.98	2.17	2.19	2.664
	3.12	0.99	2.28	2.3	2.671
	9.5	1.02	1.89	1.91	2.682
	12.3	1.66	2.1	2.13	2.684
	15.9	0.69	2.3	2.32	2.674
	16.9	2.02	1.97	2.01	2.691
BH-03	24.91	2.53	2.09	2.14	2.691
	1.5	3.52	1.74	1.81	-
	6.2	0.95	2.07	2.09	2.661
	18.2	7.48	2.18	2.34	2.741
	21.35	1.25	2.05	2.07	2.674
	25.9	0.92	2.09	2.1	2.67
	27.25	0.85	2.13	2.15	2.672
BH-04	33.4	1.78	2.11	2.15	2.68
	14.4	1.01	2.18	2.2	2.697
	17.1	2.93	2.2	2.26	2.732
	24.15	5.12	2.45	2.57	2.74
	29.23	4.92	2.06	2.16	2.694
BH-05	13.7	5.23	2.04	2.15	2.674
	18.3	6.11	2.07	2.15	2.734
	45	3.13	2.01	2.07	2.724
BH-06	1.9	7.74	2.11	2.27	2.727
	6.5	5.5	2.05	2.16	2.684
	16.7	0.6	2.23	2.25	2.715
	29.1	4.3	2.14	2.24	2.684
BH-07	3.3	5.38	2.03	2.14	2.684
	22.7	4.68	2.04	2.14	2.695
	29.5	6.5	2.33	2.48	2.734
BH-08	4.65	4.32	2.16	2.25	-
	15.3	5.41	2.13	2.24	-
	22.5	5.44	2.1	2.21	-
	27	3.81	2.01	2.09	2.672
BH-09	1.2	0.98	2.01	2.03	2.67
	15.4	3.48	2	2.07	2.741
	28.7	2.69	2.1	2.16	2.674
BH-10	3.5	5.09	2.04	2.14	-
	12.7	5.36	2.1	2.21	-
	18	10.2	2.21	2.44	-
	20.22	8.4	2.06	2.23	2.746
	26.1	2.94	2.11	2.17	2.671
BH-11	1.1	2.2	2.5	2.56	2.675
	16.7	3.79	2.18	2.27	-
	19.5	7.81	1.87	2.02	-
	26.1	1.59	2.38	2.42	-
	28.5	1.25	2.46	2.49	-

The integration of datasets of ERT profiles and boreholes is shown in Figure 7. The interpreted weak zones in the limestone bed are shown on the base map of the study area. It is visualized that the weak zones are concentrated in the north, northwest, and central regions. The region containing weak zones is highlighted with a polygon outlined with dashed lines (Figure 7). The voids in the north and northwest are relatively shallow than in the central region (Table 2 and Figure 7).

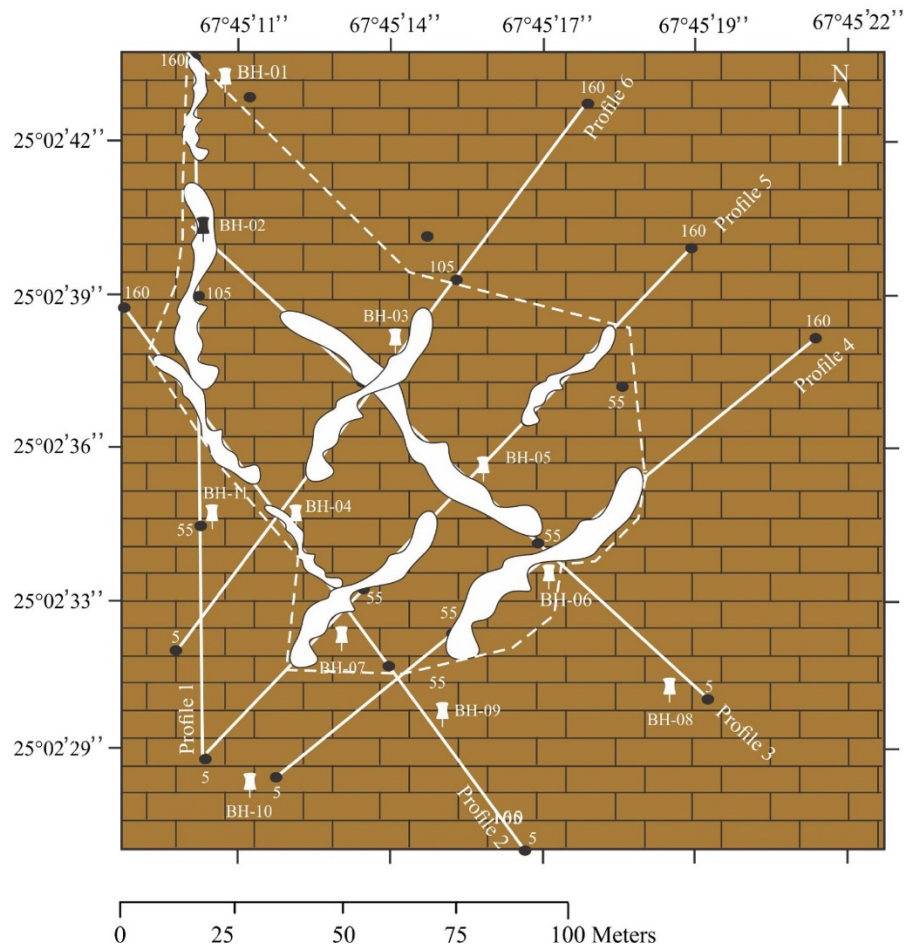


Fig. 7. The voids in limestone delineated using boreholes and ERT datasets are presented on location map of the study area.

5. Conclusion

The ERT Profiles were well-constrained with the borehole dataset and geotechnical analysis of the core samples to map subsurface weak zones. The voids identified by borehole and ERT datasets are relatively shallower in the northwestern region than in the northern and central regions of the study area. In the central region, the voids are relatively large in size, and their thickness may range from about 8-12 m. These weak zones may cause ground instability and hazard to future construction and development projects of mega infrastructure.

References

- Alle, I. C., Descloitres, M., Vouillamoz, J. M., Yalo, N., Lawson, F. M. A., & Adihou, A. C. (2018).** Why 1D electrical resistivity techniques can result in inaccurate siting of boreholes in hard rock aquifers and why electrical resistivity tomography must be preferred: the example of Benin, West Africa. *Journal of African Earth Sciences*, 139: 341-353
- André, L., E.Lamya, E., P.Lutz, P., Pernier, M., Lespinard, O., Pauss, A., & Ribeiro, T. (2016).** Electrical resistivity tomography to quantify in situ liquid content in a full-scale dry anaerobic digestion reactor. *Bioresource Technology*, 201: 89-96
- Butchibabu, B., Khan, P. K., & Jha, P. C. (2019).** Foundation evaluation of underground metro rail station using geophysical and geotechnical investigations. *Engineering Geology*, 248: 140-154
- Cueto, M., Olona, J., Fernández-Viejo, G., Pando, L., & López-Fernández, C. (2018).** Karst-induced sinkhole detection using an integrated geophysical survey: a case study along the Riyadh Metro Line 3 (Saudi Arabia). *Near Surface Geophysics*, 16(3): 270-281
- Ewusi, A., Kuma, S. J., & Voigt, H. J. (2009).** Utility of the 2-D Multi-Electrode Resistivity Imaging Technique in Groundwater Exploration in the Voltaian Sedimentary Basin, Northern Ghana. *Natural Resources Research*, 18(4): 267-275
- Hussain, Y., Ullah, S. F., Akhter, G., & Aslam, A. Q. (2017).** Groundwater quality evaluation by electrical resistivity method for optimized tubewell site selection in an ago-stressed Thal Doab Aquifer in Pakistan. *Modeling Earth Systems and Environment*, 3(1): 7-15
- Kearey, P., Michael B., & Ian H., (2002).** An introduction to Geophysical Exploration Chapter No. 08, Electrical surveying, pp. 183
- Khalil, M. H., & Hanafy, S. (2016).** Geotechnical Parameters from Seismic Measurements: Two Field Examples from Egypt and Saudi Arabia. *Journal of Environmental and Engineering Geophysics*, 21(1): 13-28
- Khan, M. J., & Ali S., (2020).** Delineation of Uncertainties in Anisotropic Shallow Subsurface by Integrated Geophysical and Geotechnical Examination. *Pakistan Journal of Science*, 72 (1): 61-67
- Li, Z. T., Ming, Q. Li, & Hong Z., (2020).** Integrated physical detection technology in complicated surface subsidence area of mining area. *Kuwait Journal of Sciences*, 47(1): 86-96.

Quraishi, I. H., Shah, S. A. A., Tariq, M. A., Khan, M. S., Ahsan, S.N., & Khanzada, M.L. (2001). Geological map of Karachi area, Sindh Pakistan: Geological Survey of Pakistan, 3

Rasul, H., Zou, L., & Olofsson, B. (2018). Monitoring of moisture and salinity content in an operational road structure by electrical resistivity tomography. *Near Surface Geophysics*, 16(4), 423-444

Redhaounia, B., Bédir, M., Gabtni, H., Batobo, O. I., Dhaoui, M., Chabaane, A., & Khomsi, S. (2016). Hydro-geophysical characterization for groundwater resources potential of fractured limestone reservoirs in Amdoun Monts (North-western Tunisia). *Journal of Applied Geophysics*, 128: 150-162

Régnier, J., Cadet, H., & Bard, P. Y. (2016). Empirical quantification of the impact of nonlinear soil behavior on site response. *Bulletin of the Seismological Society of America*, 106(4): 1710-1719

Robinson, E.S., & Coruh, C. (1988). *Basic Exploration Geophysics*. John Wiley & Sons, New York, Pp. 462

Shah, M. I. (2009). Stratigraphy of Pakistan, *GSP Memoirs*, 22: Pp. 5-6

Tao, Z., Li, M., Zhu, C., He, M., Zheng, X., & Yu, S. (2018b). Analysis of the Critical Safety Thickness for Pretreatment of Mined-Out Areas Underlying the Final Slopes of Open-Pit Mines and the Effects of Treatment. *Shock and Vibration*, 18: 1-8

Zhu, J. C., Currens, J., & Dinger, J. S. (2011). Challenges of using electrical resistivity method to locate karst conduits-a field case in the inner Bluegrass region, Kentucky. *Journal of applied Geophysics*, 75 (3): 523-530

Submitted: 18/06/2021

Revised: 14/09/2021

Accepted: 13/10/2021

DOI: 10.48129/kjs.14773